

A DSP-Based DS-CDMA Multiuser Receiver Employing Partial Parallel Interference Cancellation

Neiyer S. Correal, *Student Member, IEEE*, R. Michael Buehrer, *Member, IEEE*, and Brian D. Woerner, *Member, IEEE*

Abstract— The implementation of advanced DS-CDMA receivers based on multiuser detection principles is becoming a reality thanks to the combination of an improved understanding of the theoretical basis of multiuser detection and advances in digital, mixed-signal, and RF technologies. Due to their lower complexity, subtractive interference cancellation approaches are attractive for the practical implementation of multiuser detection. In a parallel interference cancellation receiver, it is practical to use the soft outputs of a matched filter bank for amplitude estimation. A bias arises in the decision statistics, however, due to imperfect estimation and interference cancellation. In this paper, the source of the bias is explicitly recognized, and a partial interference cancellation scheme that mitigates the negative effects of biased estimation and significantly improves system performance is proposed. A practical real-time algorithm that significantly reduces the implementation complexity of this scheme without sacrificing performance is then derived. To facilitate a software radio implementation, the signal processing complexity of the approach is characterized. The real-time processing algorithm is tested via implementation in software on a floating-point general-purpose DSP. The prototype includes a flexible software-based architecture which performs IF sampling and uses digital downconversion prior to baseband processing. The hardware test setup is described, and the results are presented and compared with simulation and analytical results. The experimental results confirm the simulation and analytical results which show large performance gains over the conventional matched filter.

Index Terms— CDMA, interference cancellation, joint detection, multiuser detection, software radios, spread spectrum.

I. INTRODUCTION

THE advent of software radio technology makes possible the implementation of highly flexible receiver architectures that employ sophisticated signal processing algorithms such as those required for multiuser detection and interference cancellation in DS-CDMA systems.

Multiuser interference cancellation techniques exploit the structured nature of the multiple-access interference (MAI), and thus offer significant gains in capacity and near-far resistance over the conventional DS-CDMA receiver. The optimal multiuser detector [1], however, is far too complex

for practical implementation in most applications. Alternate lower complexity suboptimal multiuser receiver structures that offer significant improvements over the conventional receiver have been proposed [2]–[4]. For the most part, the elevated degree of complexity has restricted these ideas to the realm of simulation, with most simulations performed under rather idealized conditions.

Our intent is to develop a practical implementation of an advanced DS-CDMA receiver based on multiuser detection principles. In previous work, we have examined the performance of several major receiver structures for a variety of situations and channel conditions. Comparative performance and computational complexity results based on theoretical and simulation analyses have been presented in [5]. Fig. 1 shows the probability of bit error versus the number of users K for several multiuser detection schemes. For a practical implementation, the multistage parallel interference cancellation approach of [6] is attractive in terms of performance, computational complexity, and robustness to moderate phase jitter and synchronization errors [7].

In order to minimize the complexity of an interference cancellation receiver, a matched filter bank is commonly used at each stage for estimation of the transmitted bits and received signal energies. Regeneration and complete subtraction of the estimated MAI is then performed to reduce the interference affecting each user. However, straightforward implementation of parallel interference cancellation results in biased decision statistics. In this paper, the source of the bias is explained, and an effective, yet simple technique for mitigating the effects of the bias and increasing performance is introduced.

Part of the power behind the concept of software radio is that it allows innovative algorithms and their implementation to be considered in an integrated manner. In this paper, a practical real-time implementation of a coherent and a noncoherent multiuser detector based on the proposed parallel partial cancellation approach is presented, along with experimental tests that confirm significant performance improvements over the conventional receiver. The austerity of the receiver and its affinity with traditional DS-CDMA demodulators embodies a fundamental design principle of our implementation. The idea is to simplify the practical application of the joint detection principles described in this paper to future commercial DS-CDMA systems. Extension to multisensor reception can be accomplished via integration with a flexible multisensor testbed. This flexible testbed was constructed for adaptive antenna and multiuser algorithm development. While this work

Manuscript received December 1997; revised February 3, 1998, June 11, 1998, and August 5, 1998. This work was supported by the Defense Advanced Research Projects Agency's Global Mobile Information Systems (GloMo) Program under Contract JFBI-94219, the Office of Naval Research under Contract 65236-97-K-7806, and the Bradley Fellowship Program.

N. S. Correal and B. D. Woerner are with the Mobile and Portable Radio Research Group, Virginia Polytechnic Institute and State University, Blacksburg, VA 24061-0350 USA.

R. M. Buehrer is with Bell Laboratories' Wireless Communication Laboratory, Whippany, NJ 07981 USA.

Publisher Item Identifier S 0733-8716(99)02985-6.

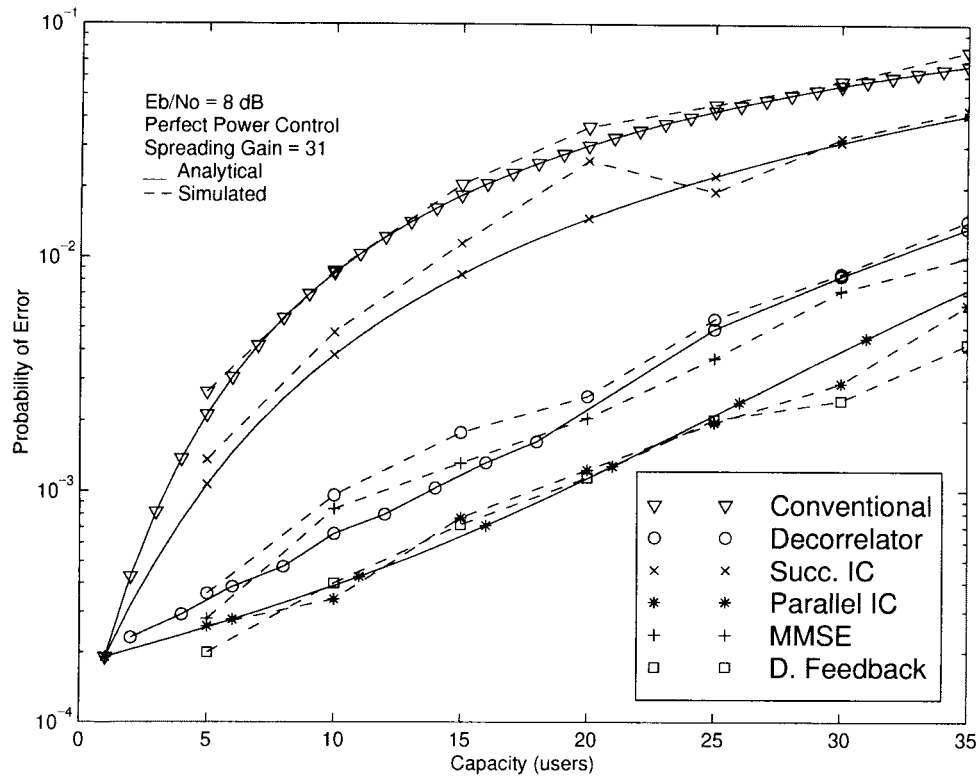


Fig. 1. Multiuser receiver probability of bit error versus number of users K (AWGN, $E_b/N_o = 8$ dB, and $N = 31$).

considers only a single antenna element, the algorithms could be extended to multiple antennas.

This hardware prototype has been developed as part of the Defense Advanced Research Projects Agency (DARPA)'s Global Mobile Information Systems (GloMo) initiative [8]. This implementation is, to our knowledge, the first working prototype of this technique. An FPGA-based parallel interference cancellation receiver has also been developed [9]. An implementation of the successive interference cancellation approach is underway at Rutgers' WINLAB [10]. A two-user DS-CDMA parallel interference cancellation hardware demonstrator is currently under development at the Swiss Federal Institute of Technology's Communication Technology Laboratory [11]. An ASIC-based approach to interference cancellation is being pursued at CEA-LETI [12]. Development activities are also underway at a number of research institutes.

Section II introduces the DS-CDMA model used in the analysis. The source of the bias is presented in Section III, along with a description and analysis of the multistage parallel partial interference cancellation technique. Section IV introduces a technique for significantly reducing the complexity of the multistage approach, and describes a noncoherent variation of the approach. Section V presents the real-time baseband processing algorithms, along with the hardware test setup. Section VI contains experimental results obtained with the real-time system. Conclusions are presented in Section VII.

II. SYSTEM MODEL

This section describes the DS-CDMA multiple-access model used in this paper. It is similar to the model described in [13].

The k th user's received signal has the form

$$\sum_{l=1}^{L_k} s_k(t - \tau_{k,l}) = \sum_{l=1}^{L_k} \sqrt{2P_{k,l}} b_k(t - \tau_{k,l}) \cdot a_k(t - \tau_{k,l}) \cos(\omega_c t + \phi_{k,l}) \quad (1)$$

where $P_{k,l}$ is the received signal power of the k th user's l th multipath component; $a_k(t)$ and $b_k(t)$ are the spreading and data waveforms, respectively (assume rectangular pulses for both, a spreading gain of N chips per bit, and completely random spreading waveforms); L_k is the number of resolvable paths for user k ; $\tau_{k,l}$ is a time delay that accounts for the asynchronous nature of the system uplink and the arrival times of the different multipath components; and $\phi_{k,l}$ is the received phase of the k th user's l th multipath relative to some arbitrary reference phase. Note that, while typical developments of multiuser algorithms assume code-on-pulse spreading (the code period equals the symbol period), interference cancellation does not require it since, for each symbol, interference cancellation can be directly implemented at the chip level. Commercial DS-CDMA systems such as IS-95 typically use long PN spreading codes, thus making the algorithm particularly practical. The received signal $r(t)$ is given by

$$r(t) = \sum_{k=1}^K \sum_{l=1}^{L_k} s_k(t - \tau_{k,l}) + n(t) \quad (2)$$

where K is the number of users, and there is a single noise source $n(t)$ from a common front end. The decision metrics $Z_{k,l,i}^{(s+1)}$ for the i th bit of the k th user in the l th path after

s stages of cancellation for an S -stage parallel cancellation scheme can be expressed as

$$Z_{k,l,i}^{(s+1)} = \int_{iT+\tau_{k,l}}^{(i+1)T+\tau_{k,l}} \hat{r}_{k,l}^{(s)}(t) a_k(t - \tau_{k,l}) \cos(\omega_c t + \phi_{k,l}) dt \quad (3)$$

where the received signal $\hat{r}_{k,l}^{(s)}(t)$ for the l th path of user k at stage s is estimated according to

$$\hat{r}_{k,l}^{(s)}(t) = r(t) - \sum_{j=1}^K \sum_{\substack{\lambda=1 \\ \lambda \neq i | j=k}}^{L_k} \hat{s}_{j,\lambda}^{(s)}(t) \quad (4)$$

and the signal $\hat{s}_{j,\lambda}^{(s)}(t)$ corresponds to the estimated signal for path λ of user j at stage s . This signal is reconstructed according to

$$\hat{s}_{k,\lambda}^{(s)}(t) = \frac{2}{T} a_k(t - \tau_{k,\lambda}) \cos(\omega_c t + \phi_{k,\lambda}) \cdot \sum_{i=-\infty}^{\infty} |Z_{k,\lambda,i}^{(s)}| b_{k,i}^{(s)} p_T(t - iT - \tau_{k,\lambda}) \quad (5)$$

where $b_{k,i}^{(s)}$ is the i th bit estimate for user k at stage s , and $p_T(t)$ is a unit pulse function of duration T equal to the bit period. The bit estimates $b_{k,i}^{(s)}$ are computed via maximal ratio combining of the decision metrics from the L_k resolvable multipath components:

$$b_{k,i}^{(s)} = \text{sgn} \left[\sum_{l=1}^{L_k} \hat{\alpha}_{k,l,i} * Z_{k,l,i}^{(s)} \right] \quad (6)$$

where $\hat{\alpha}_{k,l,i}$ is an estimate of the multipath attenuation coefficient $\alpha_{k,l,i}$.

III. ANALYSIS OF BIAS IN THE DECISION STATISTICS

In this section, the decision statistic for the direct parallel interference cancellation structure is derived. From the derivation, the existence of a bias in the decision statistics that arises due to MAI and imperfect cancellation becomes apparent.

In a direct implementation of multistage parallel interference cancellation, estimates of each user's received signal are computed at each stage in parallel by attempting to *completely* subtract out from the received signal the estimated MAI from all other users. Improved estimates can then be obtained from each of the updated user signals with reduced MAI. This process can be repeated iteratively in multiple stages.

One of the major concerns in practical implementations of multiuser receivers is computational complexity. In our implementation, a bank of matched filters is used, at each stage, for soft joint estimation of the transmitted bits and the received signal amplitudes in order to lessen the overall complexity of the multistage parallel cancellation receiver. Complete subtraction of the estimated MAI reduces the multiple-access interference affecting each user. A side benefit of this approach is its analytical tractability.

The performance of the soft-decision approach can be further improved by using a moving average estimator for the received amplitudes, where the length of the window is determined by the coherence time of the channel [14]. The use of separate adaptive channel estimation algorithms can

lead to enhanced performance. In [15], adaptive channel estimation filters significantly improve the quality of the channel coefficient estimates with moderate additional complexity.

As is shown below, straightforward implementation of parallel interference cancellation based on complete subtraction results in biased decision statistics. The bias has its strongest effect on the decision statistics in the first stage of interference cancellation. In subsequent stages of cancellation, the influence of the bias diminishes. However, if this bias leads to incorrect cancellation at the first stage, the residual effects of these errors may be observed at subsequent stages.

For clarity, first consider a two-user ($K = 2$) system with no multipath. The path subscript l is then omitted to simplify notation. Since only relative delays and phases are important, set $\phi_1 = 0$, $\tau_1 = 0$, $\phi_2 = \phi$, and $\tau_2 = \tau$. Following the notation of [16] and [17], the decision statistic at stage $s = 1$ (i.e., before any interference cancellation) for $b_i^{(1)}$, the i th bit of user 1, is

$$Z_{1,i}^{(s=1)} = T \sqrt{\frac{P_1}{2}} b_i^{(1)} + \sqrt{\frac{P_2}{2}} \cos(\phi) \left[b_{i-1}^{(2)} R_{2,1}(\tau) + b_i^{(2)} \hat{R}_{2,1}(\tau) \right] + \eta_i^{(1)} \quad (7)$$

where

$$\eta_i^{(k)} = \int_{iT+\tau_k}^{(i+1)T+\tau_k} n(t) a_k(t - \tau_k) \cos(\omega_c t + \phi_k) dt \quad (8)$$

and $R_{2,1}(\tau)$ and $\hat{R}_{2,1}(\tau)$ are the continuous-time partial cross-correlation functions of the first and second signature sequences defined by $R_{k,i}(\tau) = \int_0^T a_k(t - \tau) a_i(t) dt$ and $\hat{R}_{k,i}(\tau) = \int_{-\tau}^T a_k(t - \tau) a_i(t) dt$ for $0 \leq \tau \leq T$.

Similarly, for user 2 at stage $s = 1$, the decision statistic is given by

$$Z_{2,i}^{(s=1)} = T \sqrt{\frac{P_2}{2}} b_i^{(2)} + \sqrt{\frac{P_1}{2}} \cos(\phi) \left[b_i^{(1)} \hat{R}_{2,1}(\tau) + b_{i+1}^{(1)} R_{2,1}(\tau) \right] + \eta_i^{(2)}. \quad (9)$$

At stage 2, the estimated signal for user 2 obtained via (5) is subtracted from the received signal $r(t)$ to form a new estimated received signal for user 1 at stage 2. Using (3) to compute the decision statistic for user 1 at stage 2 leads to the expression

$$Z_{1,i}^{(2)} = Z_{1,i}^{(1)} - \frac{\cos(\phi)}{T} \left[Z_{2,i-1}^{(1)} R_{2,1}(\tau) + Z_{2,i}^{(1)} \hat{R}_{2,1}(\tau) \right]. \quad (10)$$

Substituting into (10) the expression for the decision statistics of users 1 and 2 from (7) and (9), and canceling common terms, one obtains

$$\begin{aligned} Z_{1,i}^{(2)} = & T \sqrt{\frac{P_1}{2}} b_i^{(1)} - \frac{\cos^2(\phi)}{T} \\ & \cdot \sqrt{\frac{P_1}{2}} \left[b_{i-1}^{(1)} \hat{R}_{2,1}(\tau) R_{2,1}(\tau) + b_i^{(1)} R_{2,1}^2(\tau) \right. \\ & \left. + b_i^{(1)} \hat{R}_{2,1}^2(\tau) + b_{i+1}^{(1)} R_{2,1}(\tau) \hat{R}_{2,1}(\tau) \right] \\ & + \eta_i^{(1)} - \frac{\cos(\phi)}{T} \left[\eta_{i-1}^{(2)} R_{2,1}(\tau) + \eta_i^{(2)} \hat{R}_{2,1}(\tau) \right]. \quad (11) \end{aligned}$$

Conditioning on $b_i^{(1)}$ and taking the expected value of the decision statistic yields

$$E\{Z_{1,i}^{(2)}|b_i^{(1)}\} = T\sqrt{\frac{P_1}{2}}b_i^{(1)} - \sqrt{\frac{P_1}{2}}b_i^{(1)}E\left\{\frac{\cos^2(\phi)}{T}\right\}E\left\{(R_{2,1}^2(\tau) + \hat{R}_{2,1}^2(\tau))\right\}. \quad (12)$$

For random sequences, $E\{(R_{2,1}(\tau)\hat{R}_{2,1}(\tau))\} \cong 0$; therefore, the expectation $E\{(R_{2,1}^2(\tau) + \hat{R}_{2,1}^2(\tau))\}$ in (12) can be expressed as $E\{(R_{2,1}(\tau) + \hat{R}_{2,1}(\tau))^2\}$. Equation (12) can be formulated as

$$E\{Z_{1,i}^{(2)}|b_i^{(1)}\} = T\sqrt{\frac{P_1}{2}}b_i^{(1)} - \sqrt{\frac{P_1}{2}}b_i^{(1)}E\left\{\frac{\cos^2(\phi)}{T}\right\}E\left\{(R_{2,1}(\tau) + \hat{R}_{2,1}(\tau))^2\right\}. \quad (13)$$

To evaluate this expression, note that $E\{(R_{2,1}(\tau) + \hat{R}_{2,1}(\tau))^2\}$ corresponds to the variance of $\int_0^T a_2(t-\tau)a_1(t) dt$ for a pair of randomly selected sequences since $R_{2,1}(\tau) + \hat{R}_{2,1}(\tau) = \int_0^T a_2(t-\tau)a_1(t) dt$, and $E\{(R_{2,1}(\tau) + \hat{R}_{2,1}(\tau))\} \cong 0$. The variance of this random variable (normalized for rectangular chips of period $T_c = 1$) has been shown to equal $2N/3$ using the underlying discrete cross-correlation functions [17], [18], and modeling interference as a white noise process passing through a tandem combination of two filters matched to each other [19].

Using this result and normalizing for $T_c = 1$, (13) becomes

$$E\{Z_{1,i}^{(2)}|b_i^{(1)}\} = N\sqrt{\frac{P_1}{2}}b_i^{(1)}\left[1 - \frac{1}{3N}\right]. \quad (14)$$

Since the estimates of the interfering signals are correlated with the desired user's power and bit value, a bias is produced when they are used to reconstruct and remove the interference. The bias in the mean of the decision statistics is evident in (14).

Extension of this result to a K -user system is straightforward. For K independent users with random signature sequences, following a similar approach, one obtains

$$E\{Z_{1,i}^{(2)}|b_i^{(1)}\} = N\sqrt{\frac{P_1}{2}}b_i^{(1)}\left[1 - \frac{(K-1)}{3N}\right]. \quad (15)$$

From this equation, the bias in the mean increases linearly with system loading, and is inversely proportional to the processing gain N . Similar behavior is also seen in the synchronous case [20]. However, most analyses, including our previous work [7], [21], assume independence between stages. Since the estimates of the interfering signals are correlated with the desired user's power and bit value, a bias is produced when they are used to remove the interference.

A simple yet effective way to mitigate the effect of the bias and improve the performance of a parallel multistage interference cancellation receiver is based on multiplying the channel gain estimates before signal reconstruction by a partial-cancellation factor $0 \leq C_K^{(s)} \leq 1$ that varies with the stage of cancellation s and system loading K . In this case, the

decision metric of (5) becomes

$$\hat{s}_j^{(s)}(t) = \frac{2C_K^{(s)}}{T}a_j(t)\cos(\omega_c t + \phi_j) \sum_{i=-\infty}^{\infty} Z_{j,i}^{(s)}p_T(t-iT). \quad (16)$$

This can also be interpreted as modifying the complete cancellation scheme of (4) and (5) to include the partial-cancellation factor $C_K^{(s)}$ as follows:

$$\hat{r}_k^{(s)}(t) = r(t) - C_K^{(s)} \sum_{j \neq k} \hat{s}_j^{(s)}(t). \quad (17)$$

Multiplicative factors less than 1 for interference cancellation have also been used in the derivation of an iterative approach based on maximum likelihood considerations [20], [22], mentioned in [2], and attributed to the general unreliability of the estimates at early stages.

An analysis similar to the one used earlier in this section shows that the expected value of the decision statistics of the partial interference cancellation approach is given by

$$E\{Z_{1,i}^{(2)}|b_i^{(1)}\} = N\sqrt{\frac{P_1}{2}}b_i^{(1)}\left[1 - \frac{C_K^{(2)}(K-1)}{3N}\right]. \quad (18)$$

The effect of the partial-cancellation factor on the mean and variance of the decision statistics for a two-stage parallel-cancellation receiver with $C_K^{(2)} = 0.5$ can be seen in Figs. 2 and 3, respectively. The beneficial effects of partial cancellation become apparent from a comparison with the the full-cancellation approach.

When $Z_{k,i}^{(s)}$ is an unbiased estimate, it has been shown in [21], employing the standard Gaussian approximation, that in an AWGN channel, the analytical bit-error performance of the multistage parallel-cancellation approach for user k at stage s for BPSK is

$$P_k^{(s)}(E) = Q\left(\left[\frac{1}{2E_b/N_o} \left(\frac{1 - \left(\frac{K-1}{3N}\right)^s}{1 - \frac{K-1}{3N}}\right) + \frac{1}{(3N)^s} \cdot \left(\frac{(K-1)^s - (-1)^s}{K} \cdot \left(\frac{\sum_{j \neq k} P_j}{P_k} + (-1)^s\right)\right)^{-1/2}\right]\right) \quad (19)$$

where K is the number of users and N is the processing gain.

Fig. 4 shows the probability of bit error versus the number of users K (with random spreading codes) for the complete-cancellation approach, the partial-cancellation approach, and the analytical results for the case of unbiased estimation. For these simulations, a suboptimal implementation of the partial-cancellation approach was employed. In it, the

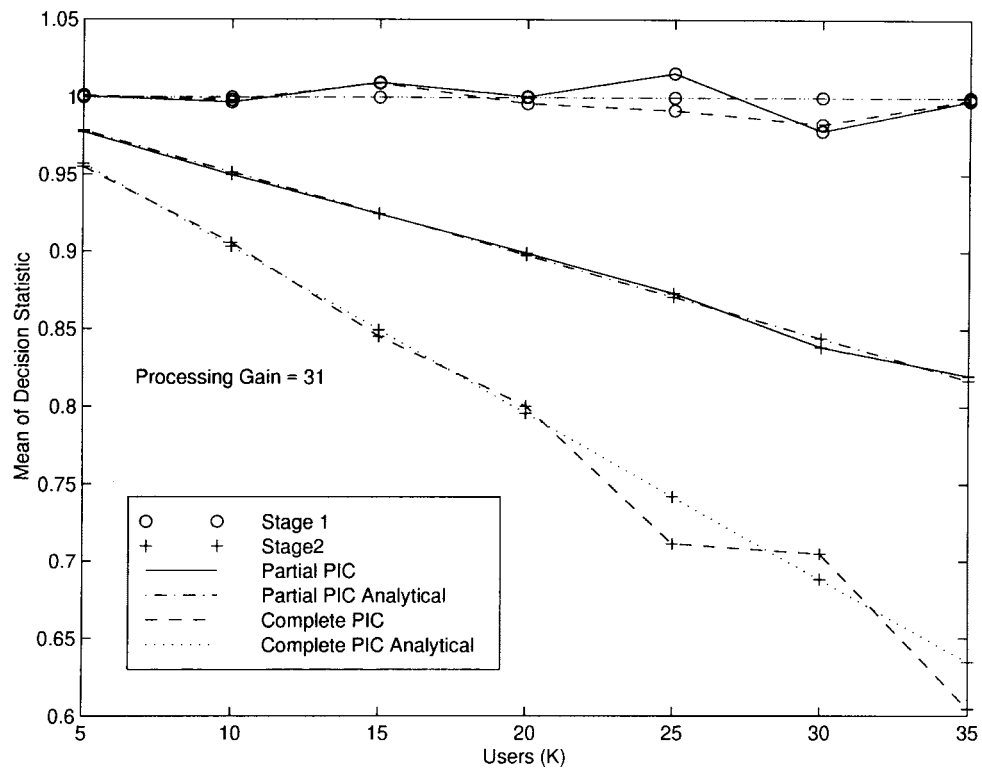


Fig. 2. Analytical and simulation results for the mean of the decision statistics for a two stage receiver using complete cancellation, and the proposed partial cancellation technique with $C_K^{(2)} = 0.5$. ($N = 31, N_o = 0$).

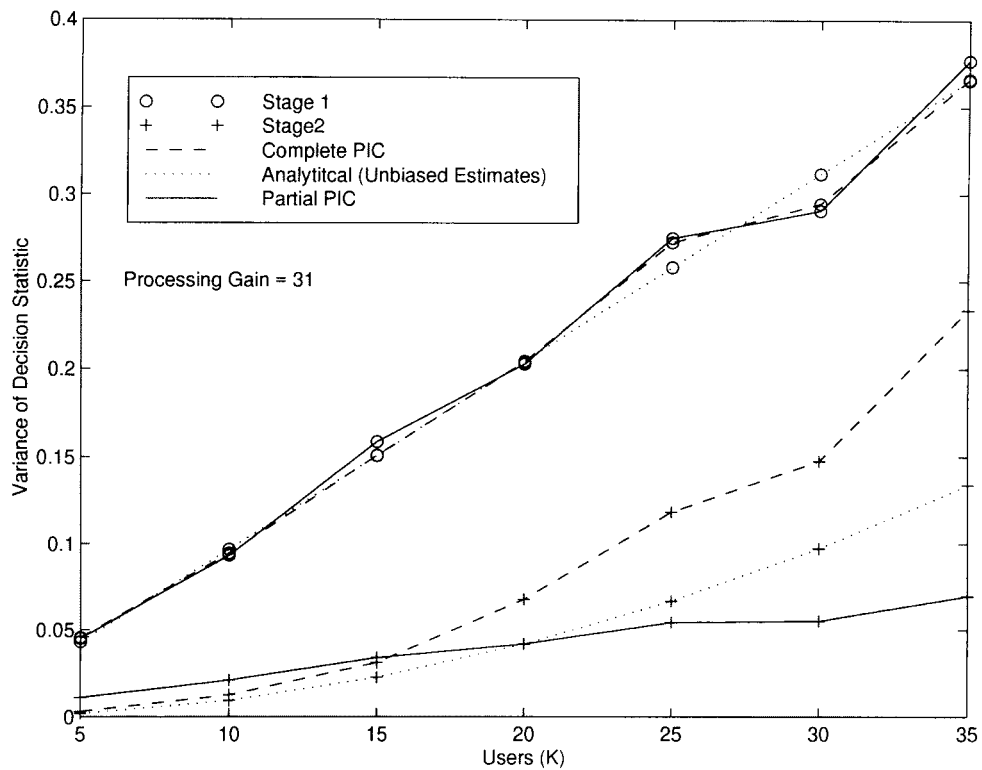


Fig. 3. Variance of the decision statistics for the direct complete cancellation, and the proposed partial interference cancellation technique with $C_K^{(2)} = 0.5$ for a two stage receiver ($N = 31, N_o = 0$).

partial-cancellation receiver uses a single constant partial-cancellation factor for the first stage of cancellation (in this case, $C_K^{(2)} = 0.5$), and in the following stages performs

complete cancellation. The justification for this approach is that the bias varies from stage to stage as $(-K/3N)^s$. Thus, in stages $s > 2$, bias mitigation is practically unnecessary.

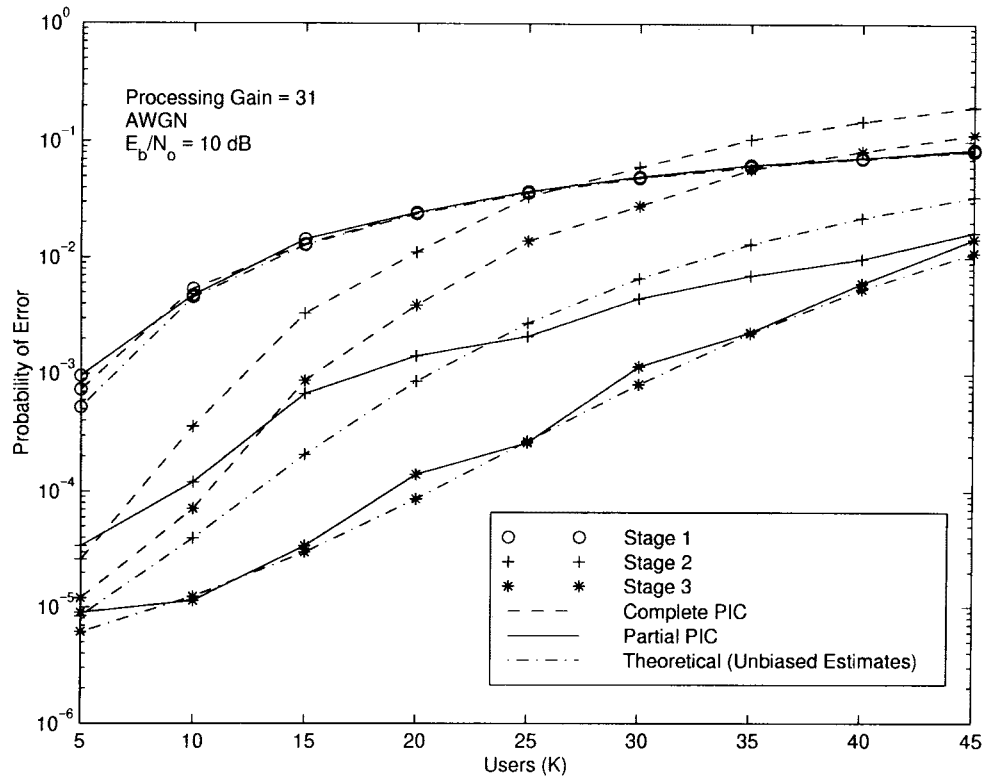


Fig. 4. Simulated probability of bit error versus number of users K for the complete parallel cancellation and the partial parallel interference cancellation approach used in the DSP implementation ($E_b/N_o = 10$ dB, and $N = 31$, with $C_K^{(2)} = 0.5$ and $C_K^{(3)} = 1$).

Comparison of the capacity curves shows that use of the proposed receiver structure results in significant performance improvements over the full parallel cancellation approach. In fact, the results for the third stage of the proposed receiver are very close to those that would be obtained with unbiased estimation. The significant improvements in capacity offered by the partial-cancellation approach are evident.

Another example of enhancement in performance offered by the partial-cancellation technique over the complete-cancellation implementation is observed in Fig. 5. Both receivers make use of Rake receivers and maximal ratio combining. The channel is a two-ray frequency-selective Rayleigh fading channel with parameters taken from measurement data presented in [23], and that correspond to one strong main path and a weak second path ($\sigma_1 = 0.93$ and $\sigma_2 = 0.28$). The partial-cancellation factor for the second stage is 0.5, and the third stage performs complete cancellation. Fig. 5 shows that, for these conditions, two stages of the partial-cancellation technique provide better performance than three stages of the direct approach. Also, after three stages of interference cancellation, the simplified partial-cancellation technique achieves about one order-of-magnitude improvement in BER compared to the direct implementation.

In many situations, the near-far effect can be a limiting factor of a DS-SS receiver's performance. In order to analyze the near-far resistance of the proposed technique, performance is examined for three desired users in the presence of a fourth user whose power varies from 20 dB below the power of the desired users to 30 dB above. Fig. 6 shows that, over a wide range of power disparities, the proposed

scheme shows near-far robustness. It is also interesting to note that, even though the near-far resistance of the second stage of the proposed receiver is inferior to that of direct interference cancellation, in stage 3, the proposed scheme reaps the benefits of bias mitigation and outperforms the direct approach.

Until now, we have assumed that the receiver structure under study achieves and maintains perfect symbol synchronization during operation. In a more realistic scenario, however, this assumption does not hold, and the decision statistics are adversely affected by clock instabilities, propagation channel uncertainties, and movement of the radios. Fig. 7 shows the effect of delay estimation errors on the performance of the proposed receiver. The estimation error is assumed to be a Gaussian random variable of zero mean and a given standard deviation measured in fractions of a chip. The simulation results indicate that the proposed receiver structure displays robustness to moderate synchronization and timing errors. A more detailed analysis of the effects of timing and phase synchronization errors for the multistage parallel cancellation approach is given in [7].

IV. A REDUCED-COMPLEXITY STRATEGY FOR MULTISTAGE PARALLEL INTERFERENCE CANCELLATION

Computational complexity is one of the main issues that affect the selection of a multiuser detection algorithm for real-time implementation. Although subtractive interference cancellation multiuser receivers are computationally efficient relative to other approaches, the parallel-cancellation approach

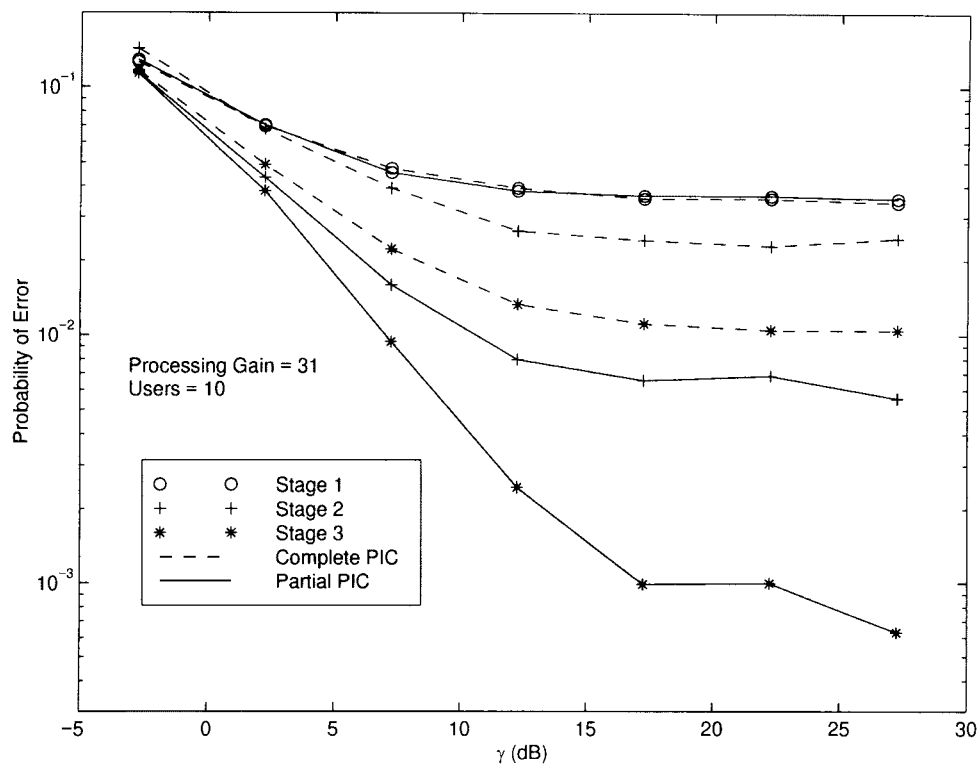


Fig. 5. BER versus average E_b/N_o comparison between complete cancellation and partial cancellation (with $C_K^{(2)} = 0.5$ and $C_K^{(3)} = 1$) for a 2-ray frequency selective Rayleigh fading channel ($\sigma_1 = 0.93$ and $\sigma_2 = 0.28$, $N = 31$).

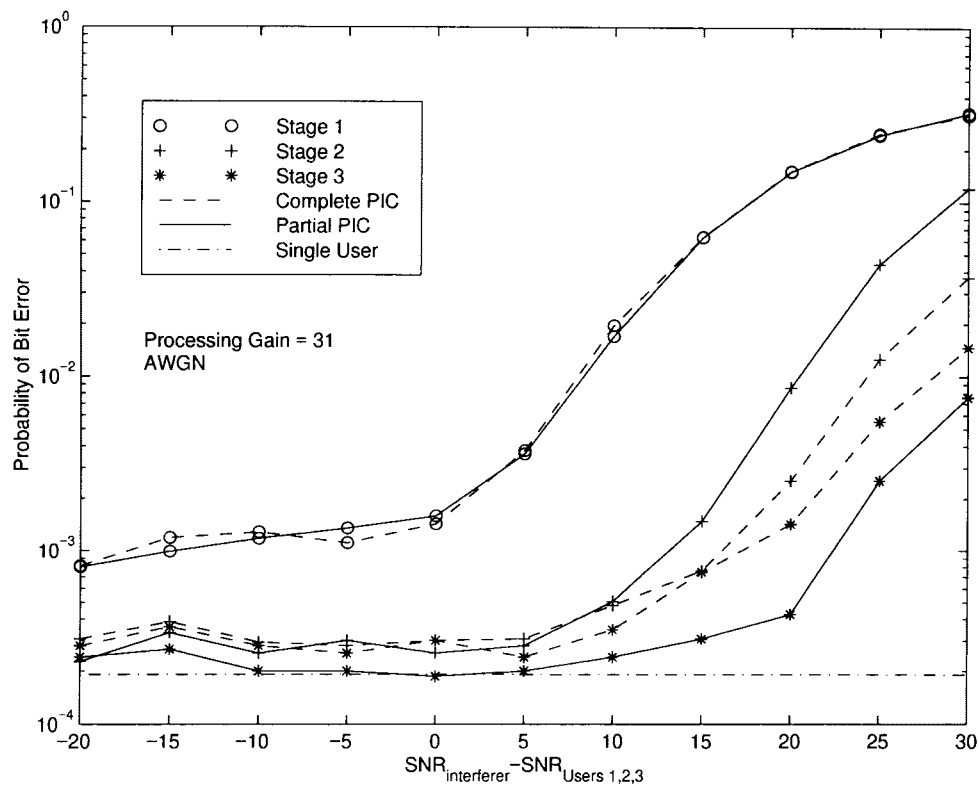


Fig. 6. BER performance degradation in near-far AWGN channels (three users with $\overline{E_b/N_o} = 8$ dB, 1 interferer with varying power. $C_K^{(2)} = 0.75$ and $C_K^{(3)} = 1$, $N = 31$).

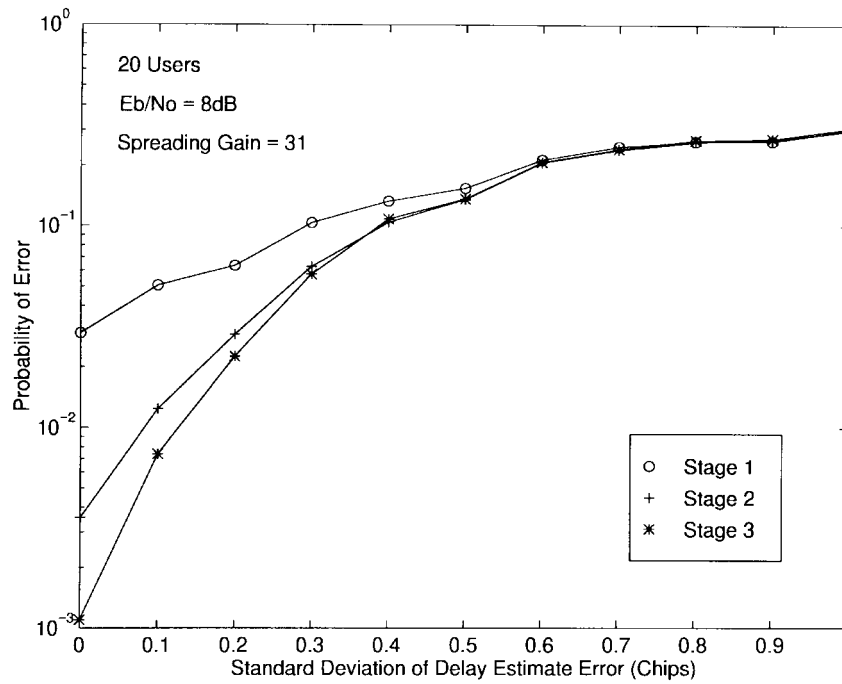


Fig. 7. Effects of symbol timing synchronization errors on system performance for partial cancellation in AWGN channels ($C_K^{(2)} = 0.5, C_K^{(3)} = 1$ and $N = 31$).

can be simplified even further. This section presents a simple technique for dramatically reducing the complexity of the decision statistics in the multistage parallel interference cancellation scheme.

A. Coherent Implementation

Coherent detection can be used when phase estimation and tracking can be performed accurately. This is may be accomplished through the use of an unmodulated auxiliary pilot signal for channel estimation. In a DSP implementation employing harmonic sampling, the input RF signal is filtered and mixed down to an intermediate frequency (IF) by an analog front end. After IF sampling, a digital downconverter, such as the Analog Devices AD6620, Harris HSP50214, or GrayChip GC1012, is then used to translate the desired signal to its baseband in-phase and quadrature (I & Q) components. For analysis and implementation of the baseband processing strategy, it is advantageous to resort to a complex-envelope representation. The baseband signal from the digital downconverters corresponds to

$$r(t) = \sum_{k=1}^K s_k(t - \tau_k) + n(t) \quad (20)$$

where the received baseband signal from user k corresponds to a binary phase-modulated waveform:

$$s_k(t) = \sqrt{P_k} a_k(t) b_k(t) e^{j\theta_k} \quad (21)$$

and θ_k is the received phase of the k th user relative to some reference phase.

In terms of the complex envelope representation, the decision statistics of (3) (now scaled by a factor of $1/T$) are

given by

$$Z_{k,i}^{(s)} = Y_{I_{k,i}}^{(s)} \cos(\theta_k) + Y_{Q_{k,i}}^{(s)} \sin(\theta_k) \quad (22)$$

where the decision metrics $Y_{I_{k,i}}^{(s)}$ and $Y_{Q_{k,i}}^{(s)}$ correspond to the I & Q outputs of a bank of matched filters for the i th bit of the k th user after s stages of cancellation. The in-phase and quadrature correlation metrics can be expressed as

$$Y_{I_{k,i}}^{(s+1)} = \frac{1}{T} \int_{(i-1)T+\tau_k}^{iT+\tau_k} \hat{r}_{I_k}^{(s)}(t) a_k(t - \tau_k) dt \quad (23)$$

$$Y_{Q_{k,i}}^{(s+1)} = \frac{1}{T} \int_{(i-1)T+\tau_k}^{iT+\tau_k} \hat{r}_{Q_k}^{(s)}(t) a_k(t - \tau_k) dt \quad (24)$$

where the received complex-baseband signal $\hat{r}_k^{(s)}(t)$ at stage s for user k is generated by subtracting from the received signal the estimated MAI from the remaining users:

$$\hat{r}_{I_k}^{(s)}(t) = r_I(t) - \sum_{j=1, j \neq k}^K \hat{s}_{I_j}^{(s)}(t - \tau_j) \quad (25)$$

$$\hat{r}_{Q_k}^{(s)}(t) = r_Q(t) - \sum_{j=1, j \neq k}^K \hat{s}_{Q_j}^{(s)}(t - \tau_j). \quad (26)$$

Signal $\hat{s}_j^{(s)}$ corresponds to the complex-valued signal for user j at stage s , reconstructed using the decision statistic $Z_{j,i}^{(s)}$ which provides a combined estimate of the data bit and the signal amplitude:

$$\hat{s}_{I_j}^{(s)}(t) = a_j(t) \sum_{i=-\infty}^{\infty} C_j^{(s)} Z_{j,i}^{(s)} p_T(t - iT) \cos(\phi_j) \quad (27)$$

$$\hat{s}_{Q_j}^{(s)}(t) = a_j(t) \sum_{i=-\infty}^{\infty} C_j^{(s)} Z_{j,i}^{(s)} p_T(t - iT) \sin(\phi_j) \quad (28)$$

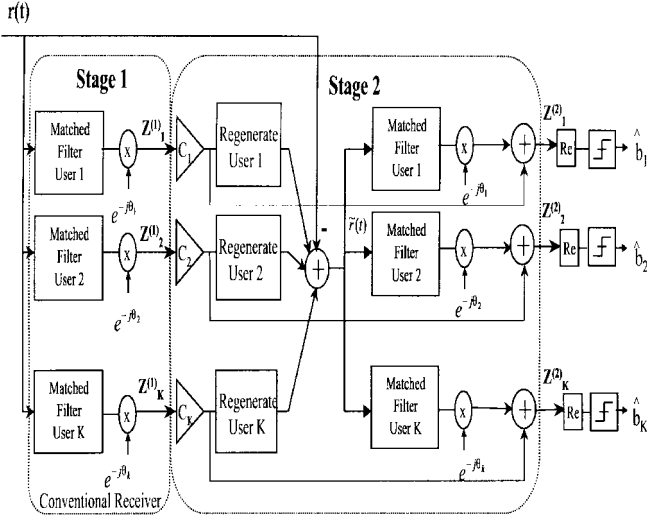


Fig. 8. Block diagram of the coherent parallel partial interference cancellation receiver.

where $C_j^{(s)}$ is the partial-cancellation multiplicative factor used for bias mitigation. This notation allows the use of a different cancellation factor for every user to optimize system performance for different channel conditions and for unequal received powers. Derivation of the optimal partial-cancellation factor has been studied in [24].

For parallel interference cancellation, the approach described by (25) and (26) is conceptually attractive since it makes the underlying idea of interference cancellation simple to understand. However, this approach also entails a computational complexity of $O(K^2)$ since, for each of the K users, reconstruction of the MAI affecting each signal is accomplished by adding the estimated signals of the remaining $K-1$ users. As the number of users increases, the complexity of this approach grows rapidly.

In our implementation, a theoretically equivalent approach reduces the complexity of the reestimation scheme to $O(K)$ [14]. A block diagram of this approach is shown in Fig. 8. The reduced-complexity approach used in the DSP implementation is summarized as follows.

First, a residual signal $\tilde{r}(t)$ is created by subtracting from the received signal the sum of the estimated received signals from *all* users

$$\hat{r}_I^{(s)}(t) = r_I(t) - \sum_{j=1}^K \hat{s}_{I_j}^{(s)}(t - \tau_j) \quad (29)$$

$$\hat{r}_Q^{(s)}(t) = r_Q(t) - \sum_{j=1}^K \hat{s}_{Q_j}^{(s)}(t - \tau_j) \quad (30)$$

where $\hat{s}_{I_j}^{(s)}(t)$ and $\hat{s}_{Q_j}^{(s)}(t)$ are defined in (27) and (28). With these definitions, $\hat{r}_{I_k}^{(s)}(t)$ and $\hat{r}_{Q_k}^{(s)}(t)$ correspond to

$$\hat{r}_{I_k}^{(s)}(t) = \hat{s}_{I_k}^{(s)}(t - \tau_k) + \tilde{r}_I^{(s)}(t) \quad (31)$$

$$\hat{r}_{Q_k}^{(s)}(t) = \hat{s}_{Q_k}^{(s)}(t - \tau_k) + \tilde{r}_Q^{(s)}(t). \quad (32)$$

Substituting these expressions into (23) and (24) gives

$$Y_{I_{k,i}}^{(s+1)} = \frac{1}{T} \int_{(i-1)T+\tau_k}^{iT+\tau_k} (\hat{s}_{I_k}^{(s)}(t - \tau_k) + \tilde{r}_I^{(s)}(t)) a_k(t - \tau_k) dt \quad (33)$$

$$Y_{Q_{k,i}}^{(s+1)} = \frac{1}{T} \int_{(i-1)T+\tau_k}^{iT+\tau_k} (\hat{s}_{Q_k}^{(s)}(t - \tau_k) + \tilde{r}_Q^{(s)}(t)) a_k(t - \tau_k) dt. \quad (34)$$

Substituting the definitions of (27) and (28) for the reconstructed signals $\hat{s}_{I_k}^{(s)}(t)$ and $\hat{s}_{Q_k}^{(s)}(t)$ of user k into the previous equations, the decision statistics after s stages of cancellation in (33) and (34) reduce to

$$Y_{I_{k,i}}^{(s+1)} = C_k^{(s)} Z_{k,i}^{(s)} \cos(\theta_k) + \frac{1}{T} \int_{(i-1)T+\tau_k}^{iT+\tau_k} \tilde{r}_I^{(s)}(t) a_k(t - \tau_k) dt \quad (35)$$

and

$$Y_{Q_{k,i}}^{(s+1)} = C_k^{(s)} Z_{k,i}^{(s)} \sin(\theta_k) + \frac{1}{T} \int_{(i-1)T+\tau_k}^{iT+\tau_k} \tilde{r}_Q^{(s)}(t) a_k(t - \tau_k) dt. \quad (36)$$

The improved decision statistics are computed according to (22) using the decision statistics $Z_{k,i}^{(s)}$ obtained in the previous stage and a correction factor that is computed using the complex-valued residual signal $\tilde{r}(t)^{(s)}$

$$Z_{k,i}^{(s+1)} = C_k^{(s)} Z_{k,i}^{(s)} + \text{Re} \left[\int_{(i-1)T+\tau_k}^{iT+\tau_k} \tilde{r}^{(s)}(t) a_k(t - \tau_k) e^{-j\phi_k} dt \right]. \quad (37)$$

The dramatic reduction in computational complexity over the straightforward full-cancellation approach of (25) and (26) stems from the fact that the residual signal is identical for all users, and thus needs to be generated only once per stage.

B. Noncoherent Implementation

An implementation of the proposed receiver that does not require a coherent phase reference and employs differentially encoded BPSK has also been developed. The notion of noncoherent multiuser demodulation of differentially phase-shift keyed DS-CDMA signals has been addressed in [25], [26], and [3]. An alternate approach based on M -ary orthogonal modulation and OQPSK has been explored in [27]. The use of differential detection and multistage parallel interference cancellation has also been addressed in [5], where a BER performance comparison is also presented for various noncoherent multiuser receivers. Here, we focus on a reduced-complexity approach for practical implementation. In this receiver, the in-phase and quadrature decision statistics of (23) and (24) are used directly for estimation of the amplitudes, symbols, and relative phases of the received signals. The approach of the noncoherent implementation is similar to that of the coherent

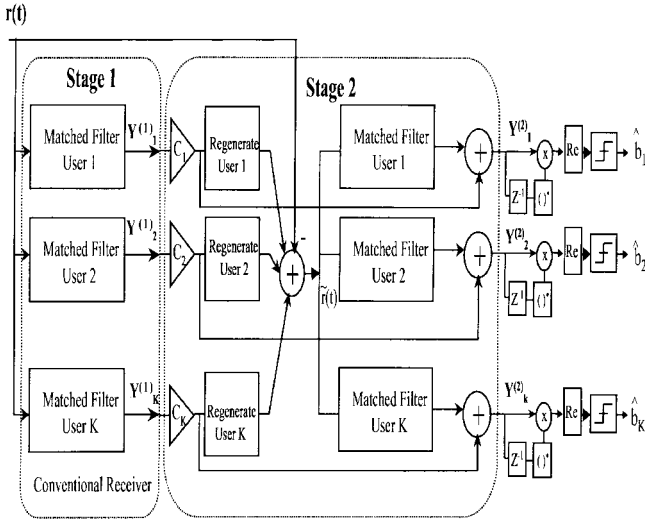


Fig. 9. Block diagram of the differentially coherent parallel partial interference cancellation receiver.

approach. A block diagram of the receiver is presented in Fig. 9.

The received baseband signal $\hat{r}_k^{(s)}(t)$ at stage s for user k is generated by subtracting from the received signal the reconstructed MAI caused by other users

$$\hat{r}_k^{(s)}(t) = r_I(t) - \sum_{j=1, j \neq k}^K \hat{s}_j^{(s)}(t - \tau_j) \quad (38)$$

$$\hat{r}_k^{(s)}(t) = r_Q(t) - \sum_{j=1, j \neq k}^K \hat{s}_j^{(s)}(t - \tau_j). \quad (39)$$

Equations (38) and (39) are introduced for the purpose of clarity. In the actual implementation of the noncoherent receiver, the previously discussed residual signal approach was also employed in order to reduce computational complexity.

The in-phase and quadrature outputs of the matched filter bank at stage s are

$$Y_{I_k,i}^{(s+1)} = \frac{1}{T} \int_{(i-1)T+\tau_k}^{iT+\tau_k} \hat{r}_k^{(s)}(t) a_k(t - \tau_k) dt \quad (40)$$

$$Y_{Q_k,i}^{(s+1)} = \frac{1}{T} \int_{(i-1)T+\tau_k}^{iT+\tau_k} \hat{r}_k^{(s)}(t) a_k(t - \tau_k) dt. \quad (41)$$

In the noncoherent implementation, the in-phase and quadrature components of the complex-valued signal $\hat{s}_j^{(s)}$ for user j at stage s are reconstructed from the decision statistics $Y_{I_j,i}^{(s)}$ and $Y_{Q_j,i}^{(s)}$ obtained in the previous stage as follows:

$$\hat{s}_{I_j}^{(s)}(t) = a_j(t) \sum_{i=-\infty}^{\infty} C_j^{(s)} Y_{I_j,i}^{(s)} p_T(t - iT) \quad (42)$$

$$\hat{s}_{Q_j}^{(s)}(t) = a_j(t) \sum_{i=-\infty}^{\infty} C_j^{(s)} Y_{Q_j,i}^{(s)} p_T(t - iT) \quad (43)$$

where $C_j^{(s)}$ is the partial-cancellation multiplicative factor used for bias mitigation for user j . Note that intrinsic information

about the user's phases is embedded in the correlation metrics $Y_{I_j,i}^{(s)}$ and $Y_{Q_j,i}^{(s)}$.

Using the residual signal, the signals $\hat{r}_k^{(s)}(t)$ and $\hat{r}_k^{(s)}(t)$ of (38) and (39) can be expressed as

$$\hat{r}_k^{(s)}(t) = \hat{s}_{I_k}^{(s)}(t - \tau_k) + \hat{r}_I^{(s)}(t) \quad (44)$$

$$\hat{r}_k^{(s)}(t) = \hat{s}_{Q_k}^{(s)}(t - \tau_k) + \hat{r}_Q^{(s)}(t). \quad (45)$$

Substituting these expressions into (40) and (41), and using the definitions of (42) and (43), the decision statistics after s stages of cancellation are reduced to

$$Y_{I_k,i}^{(s+1)} = C_k^{(s)} Y_{I_k,i}^{(s)} + \frac{1}{T} \int_{(i-1)T+\tau_k}^{iT+\tau_k} \hat{r}_I^{(s)}(t) a_k(t - \tau_k) dt \quad (46)$$

and

$$Y_{Q_k,i}^{(s+1)} = C_k^{(s)} Y_{Q_k,i}^{(s)} + \frac{1}{T} \int_{(i-1)T+\tau_k}^{iT+\tau_k} \hat{r}_Q^{(s)}(t) a_k(t - \tau_k) dt. \quad (47)$$

Decisions are made on the estimates produced by projecting the current complex-valued decision statistic onto the previous one. The phase of the resulting complex number is then used as an estimate of the phase difference between consecutive symbols

$$Z_{k,i}^{(s)} = \text{Re} \left[Y_{k,i}^{(s)} (Y_{k,i-1}^{(s)})^* \right] \quad (48)$$

In terms of the complex envelope representation, the decision statistics for differential decoding are thus given by

$$Z_{k,i}^{(s)} = Y_{I_k,i}^{(s)} Y_{I_k,i-1}^{(s)} + Y_{Q_k,i}^{(s)} Y_{Q_k,i-1}^{(s)}. \quad (49)$$

Thus, while the phase is implicitly estimated for cancellation, it is not used for detection. Fig. 10 presents BER curves as a function of the number of users in AWGN, obtained via simulation for a multistage noncoherent implementation and an ideal coherent implementation.

It is interesting to note that, as the number of users increases, the relative performance of the noncoherent receiver with respect to the coherent scheme deteriorates. This can be attributed to the degradation of the inherent phase information in the decision statistics caused by increasing levels of MAI.

C. Computational Complexity Calculations

In order to quantify the computational complexity of the algorithms for DSP implementation, we assume a processing engine capable of performing single-cycle multifunction operations and zero-overhead looping. In this processing architecture, multiply and add instructions as well as compute/move operations are performed in parallel in one processor cycle. We also assume that the processor is capable of performing multiple memory accesses per instruction cycle.

The computational complexity per bit period of the reduced-complexity algorithm can be computed in terms of the number of users K , the spreading factor N , the number of samples per chip N_s , the number of fingers in the Rake receiver L , and the number of stages S as follows.

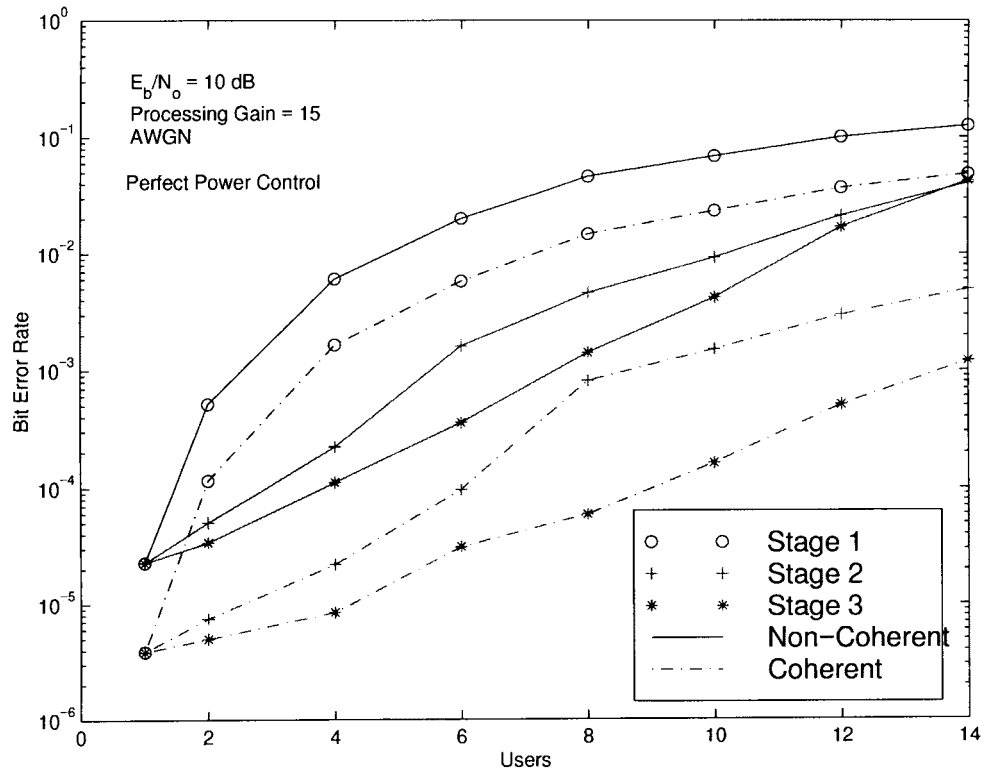


Fig. 10. Probability of bit error versus number of users for the noncoherent multiuser receiver, and for an ideal coherent implementation ($N = 15$, $C_k^{(1)} = 1.0$, $C_k^{(2)} = 0.75$ for loads ≤ 6 users and $C_k^{(2)} = 0.5$ for larger loads).

Complex baseband data acquisition, floating-point conversion, and storage require on the order of $6LNN_s$ operations. The computational burden of this task on the CPU can, however, be significantly reduced by using a separate I/O processing unit. Implementation of the correlation demodulator stage involves correlation in the I & Q arms, multiplication of the decision statistics by the conjugate of the phase, normalization by $1/(NN_s)$, and storage of the soft decision statistics. Execution of these tasks requires $2KLN_s + 28KL$ operations.

Interference cancellation involves fetching the soft decision statistics, resampling the estimated user signals, and subtraction of the respread signals from the original received signal. This requires $4KLN_s + 32KL$ operations in the case of the reduced-complexity approach, and $4(K^2 - K)LNN_s + 32(K^2 - K)L$ operations for the direct approach.

Computation of the improved decision statistics requires correlation of the residual signal with the signature sequences, normalization of the correction factors, multiplication by the conjugate of the user's phase, and addition of the correction factors to the initial decision statistics. This stage can be thought of as another correlation demodulator with computational complexity $2KLN_s + 28KL$.

In a multistage approach, implementation of multiple stages of interference cancellation and reestimation is achieved by cascading functional blocks that perform interference cancellation followed by reestimation. After the desired number of cancellation stages, the final decision statistics for the L branches are computed via maximal ratio combining, an operation which requires $5KL$ operations. Transformation of

TABLE I
ESTIMATED AND MEASURED NUMBER OF PROCESSING CYCLES REQUIRED FOR IMPLEMENTATION OF THE MAIN FUNCTIONAL TASKS FOR INTERFERENCE CANCELLATION

Task	$N_s = 4$		$N_s = 2$	
	Est.	Meas.	Est.	Meas.
Correlation	592	610	360	374
MAI Cancellation	1088	1103	612	622
Re-Estimation	592	624	360	382
Total	2272	2305	1332	1378

the soft outputs of the combiner to hard bit decisions is accomplished in K operations.

The conventional receiver, which corresponds to a correlation demodulator, has a computational complexity of $6LNN_s + 2KLN_s + 33KL + K$. For multistage parallel interference cancellation, the number of operations required with the reduced complexity implementation is approximately $6LNN_s + 2KLN_s(3S - 2) + 60KLS - 27KL + K$. The overall computational complexity of this approach is linear in the number of users. The computational complexity of the direct approach, on the other hand, corresponds to $6LNN_s + 2KLN_sS(2K - 1) + KLS(32K - 4) - 4KLN_s(K - 1) - KL(32K - 37) + K$, a computational complexity that is quadratic in the number of users K .

The preceding expressions account for the major functional tasks of the algorithm itself, and do not account for phase estimation (required for coherent detection, unnecessary with the noncoherent receiver) or synchronization and tracking. Table I compares the estimated computational complexity for the major functional blocks of the reduced-complexity algo-

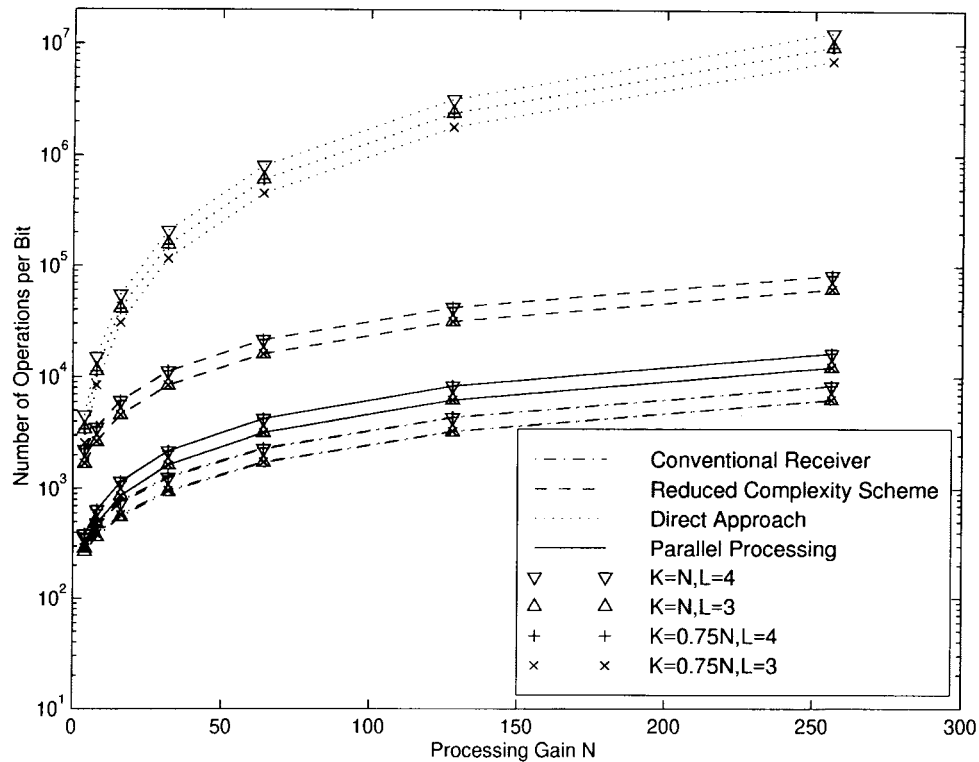


Fig. 11. Number of operations per user bit versus processing gain for system loads $K = 0.75N$ and $K = N$, for a receiver with an $L = 4$ Rake receiver, $N_s = 4$ samples per chip, and $S = 3$ stages of cancellation.

rithm with measures obtained from profiling sessions of the code running on our DSP platform with $N = 15$, $K = 4$, $L = 1$, $S = 2$, setting the number of samples per chip first to $N_s = 4$, and then to $N_s = 2$.

An advantage of the multistage parallel interference cancellation approach is that it can be efficiently implemented with multiple processors working concurrently. A data flow multiprocessing approach where data pass linearly from one processor to another, and each processor performs a different functional task, can be used to efficiently achieve the required high computational bandwidth. Another advantage of the data flow multiprocessing approach is that it results in a homogeneous scalable system, where the main processing structure is replicated multiple times according to the number of stages of interference cancellation desired.

Although the overall number of required processor cycles remains unchanged, the number of cycles required per processor is significantly reduced. In this case, the most computationally expensive functional task sets the limit in the processing pipeline. For comparison, assume that signal reconstruction and interference cancellation tasks are performed in a single processor, thus dictating the computational requirement of the reduced-complexity multiprocessor implementation.

Fig. 11 shows the number of processing operations per bit for implementation of the different algorithms as a function of processing gain N for system loads of $K = 0.75N$ and $K = N$. A receiver using an $L = 3$ and $L = 4$ Rake receiver, four samples/chip ($N_s = 4$), and three stages of processing ($S = 3$). In this graph, the advantage of using a parallel processing technique is evident, especially for highly loaded systems with large processing gains.

When compared to the classical approach for demodulating multiple users, the proposed reduced-complexity implementation does not bring about a significant increase in memory requirements. This is accomplished by using a direct bit-by-bit processing scheme as opposed to a memory-intensive block-processing approach. Due to the asynchronous nature of the multiple-access channel, buffering of contiguous bits is necessary to avoid overwriting useful data. The proposed algorithm has been successfully implemented using a processing strategy that requires a transitional processing buffer that only encompasses five bit epochs per interference cancellation stage, as opposed to two for the conventional receiver. Other intermediate results such as the correction factors and the intermediate decision statistics require very little additional memory, and can be basically ignored, to a first-order approximation.

V. HARDWARE IMPLEMENTATION

This section describes the multisensor RF and baseband demodulation segments of the hardware prototype. First, the analog section of the multisensor testbed is described. Then, a practical I/Q implementation with carefully timed data streams (to allow cancellation of asynchronous multiple access signals) is described. Experimental results follow.

A. RF Front End

A flexible multisensor testbed¹ suitable for adaptive beamforming and multiuser detection has been implemented [28]. A block diagram is seen in Fig. 12.

¹The development system contains multiple sensors for beamforming applications, but the algorithms described here are for a single antenna.

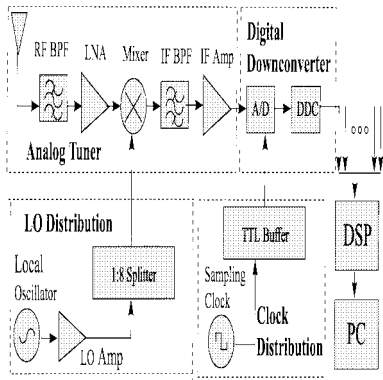


Fig. 12. Block diagram of the multisensor testbed.

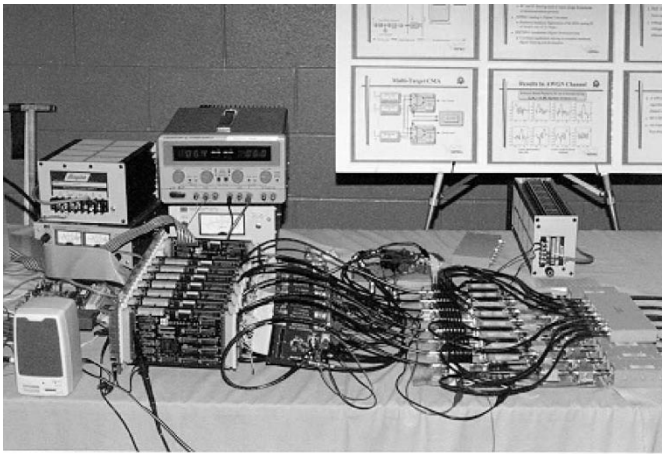


Fig. 13. RF and downconversion section of the multisensor testbed. (Courtesy of Don Breslin.)

The analog tuner downconverts signals from an RF of 2050 MHz to an IF of 68 MHz. It has a noise figure of 4 dB, and provides 75 dB of spurious free dynamic range in a 2 MHz IF bandwidth with a minimum detectable signal of -111.4 dB. Fig. 13 shows the RF front end and the downconversion stage.

The RF bandpass filter rejects out-of-band interference. It is desirable for this filter to have a low insertion loss and linear phase across the passband. The RF low-noise amplifier (LNA) increases the level of the signal before it reaches the mixer. The choice of LNA plays a key role in determining the noise figure of the receiver. Excessive gains are avoided, however, since they give rise to intermodulation and distortion in the mixing process.

Following RF amplification, the signal is mixed down to IF. A common local oscillator (LO) signal drives the mixers of all of the branches of the analog tuners. Selection of the mixer is important since distortion from the mixing process affects the receiver's dynamic range. Postmixer bandpass filtering rejects undesired out-of-band signals, mixer spurious products, and RF and LO mixer leakage.

After amplification of the analog IF signal, the IF is digitized using harmonic sampling. Several practical considerations for selecting analog-to-digital converters for harmonic sampling

applications are presented in [29]. Once the IF signal has been digitized, digital downconverters further filter and translate the band of interest to the complex baseband. By relieving the DSP from the processing burden of downconversion, more computational power becomes available for the tasks of estimation, interference cancellation, and detection. Digital downconversion not only eliminates the need for another IF stage, but it also overcomes many of the problems related to analog downconversion and low-pass digitization. Discussion of sampling, IF processing, and digital downconversion techniques are presented in [30] and [31].

B. Baseband Multiuser Demodulation Segment

In this section, the real-time asynchronous baseband multiuser demodulation segment is presented. The multiuser demodulation scheme has one stage of interference cancellation. In this system, baseband processing functions are implemented on modular Analog Devices ADSP21020 EZLAB boards. The direct-sequence BPSK system has a processing gain $N = 15$, and supports an aggregate rate of 20 kbits/s. As discussed in the previous section, after proper signal conditioning, the IF signal is downconverted, decimated, and filtered for baseband processing. The input to the signal processing segment is the complex-baseband multiple access data stream of (20). Data acquisition is interrupt driven.

Since arithmetic operations such as addition and multiplication are at the core of the algorithms used in this receiver, the performance of the algorithms is influenced by the wordlength and type of arithmetic used by the system. Fixed-point hardware is currently significantly cheaper, faster, and more power efficient than floating-point hardware. Nonetheless, following the trend in rapid prototyping, this implementation uses a 32-bit floating-point processor since floating-point arithmetic simplifies algorithm development. Optimization for fixed point can be performed from this working foundation. The performance of a fixed-point implementation of the multistage parallel interference cancellation technique has been investigated analytically and via simulations in [32].

In order to minimize the effects of timing errors, a high sampling rate is desired. On the other hand, high sampling rates increase the processing bandwidth required from the DSP's. The effects of timing errors on the performance of multistage parallel interference cancellation receivers have been studied in [7]. Analytical and simulation results indicate that multistage parallel interference cancellation receivers are fairly robust, and show moderate reductions in performance due to timing errors on the order of $T_c/8$. A rate of four samples/chip was selected as a compromise between minimizing the negative effects of synchronization errors and timing misalignment at the receiver (keeping average timing errors below $T_c/8$) and minimizing the overall computational complexity of the implementation.

The DSP section of the receiver operates on the complex-baseband signal as it arrives, which avoids unnecessary processing delays and storage requirements associated with block processing. This system takes advantage of the short length of the spreading codes by using a noncoherent matched-filter approach for initial acquisition.

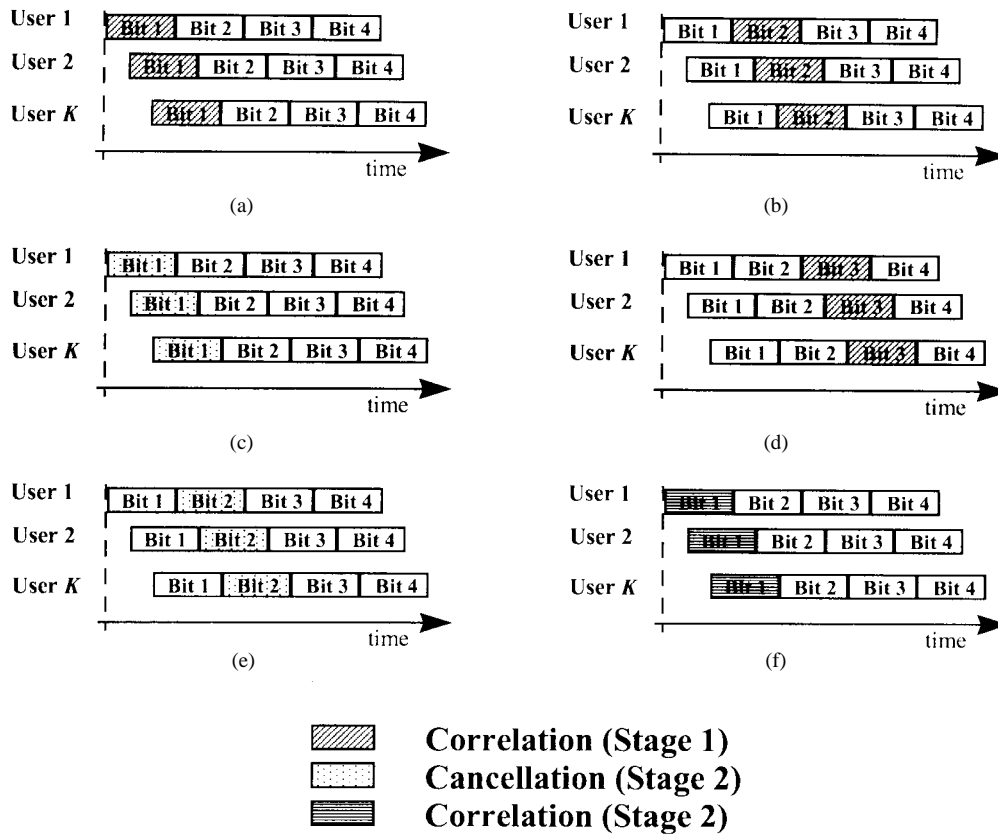


Fig. 14. Timing diagram describing the processing flow for real-time implementation.

A coherent synchronization approach that takes advantage of the multistage architecture by using the residual signal $\hat{r}(t)$ for improved acquisition and tracking has been studied in [33]. Since the residual signal has reduced levels of MAI, the probability of false alarm and mean acquisition time of the system is reduced. This technique will be incorporated in the receiver in the near future.

The processing can be described with the aid of the signal flow diagram in Fig. 8 and the timing diagram of Fig. 14. Baseband processing is based on the decision metric from (37). This metric can be applied either in continuous-time processing or by block processing. In a synchronous system, there would be no real difference between the two. However, in an asynchronous system, care must be taken in deriving the real-time processing flow. The reason for this is seen in Fig. 14. Since there is overlap between the bits of different users, one cannot process a bit in its entirety without processing the overlapping bits. A block processing scheme would be satisfactory, but it incurs a delay which is directly proportional to the block size. Another approach is to process the bits as they arrive in real time. The first step is to perform a correlation between the spreading code associated with the signal under consideration and the received signal at baseband. (It is assumed that the receiver has already locked onto the correct code phase as well as carrier phase.) This is done for the current bit of each user (arbitrarily denoted as "bit 1"). In order to ensure that enough samples have arrived for each user, one allows two data bits of any specific

user to arrive, which assures that all users have at least one bit available. Thus, the first step is to create the first stage decision statistic for bit 1 of each user [Fig. 14(a)]. This is stored and used as an estimate of each user's data bit and received power in the cancellation. Since there is overlap between bit 1 of user k and bit 2 of any user j where $j < k$ (assuming users are numbered according to increasing delays), the first-stage decision statistics of each user are needed for bit interval 2 [Fig. 14(b)] before proceeding with cancellation. Once stage 1 correlation is completed for each user over bits 1 and 2, cancellation over bit interval 1 may occur [Fig. 14(c)]. This is done by first multiplying the correlation score by the factor C_k and the spreading code of each user, and then using the resulting signal estimate to subtract out each estimated signal from the received signal. This residual signal is then stored and saved for processing in stage 2.

Due to the overlap of bit 2 and bit 1 as described in the preceding paragraph, one cannot proceed with stage 2 processing until interference has been removed from all samples affecting bit 1 of each user. Thus, interference during bit intervals 1 and 2 should be cancelled before stage 2 processing begins on bit number 1. However, as explained for bit 1, one cannot cancel interference over bit interval 2 before performing initial correlations over bit interval 3. Thus, the next step is to perform correlation over bit interval 3 [Fig. 14(d)] followed by stage 1 cancellation on bit 2 of each user [Fig. 14(e)]. Then, stage 2 processing can be performed on bit 1 [Fig. 14(f)]. In

stage 2, the residual signal is correlated with the spreading code of each user to obtain a correction factor which is added to the correlation score of the first stage as described in (37). The result is then used as the decision statistic. If additional stages are used, one recreates the estimated signals based on these new correlation scores, and creates a new residual signal using the original received samples and the new signal estimates. After stage 2 is completed, one performs correlation on bit interval 4 followed by stage 1 cancellation on bit 3 before performing stage 2 processing on bit 2. This loop continues with initial correlation performed on bit interval n , followed by stage 1 processing of bit $n - 1$, and subsequent stage 2 processing of bit $n - 2$ before starting again with bit $n + 1$ [14]. While the processing described is performed by a single DSP, it can be shown that each of the three steps can be done in parallel with proper timing. Thus, multiple slower processors can be used rather than a single high-speed processor.

VI. EXPERIMENTAL RESULTS

In order to test the real-time baseband processing segments of the DSP-based parallel interference cancellation receiver, a real-time multiple-access channel emulator was developed using an ADSP21020 EZLAB board. The baseband channel emulator takes the information that the different users wish to convey to the multiuser receiver, and creates an asynchronous complex-baseband multiuser signal stream. The channel emulator allows stipulation of the desired E_b/N_o , and the relative delays and phases among users. The delays and phases remain constant for the duration of the test. The baseband channel emulator is interfaced to the DSP baseband processing segment over the same interface that is used to receive the complex-baseband signals produced by the IF digital downconversion.

A bit-error-rate tester was developed using the multiple-access channel emulator. At the transmitter, a pseudorandom data stream is internally generated from which bits are assigned to the different users. The composite multiple-access signal is then created, and the desired level of additive white Gaussian noise (AWGN) is added. At the receiver, the received stream is decoded, and the estimated data are compared against an internally generated reference pseudorandom bit stream. The number of mismatches is measured in real time, and the measured BER is compared with those predicted by simulations.

Fig. 15 shows a comparison between the experimental BER from the real-time system and those predicted via simulation for a test with four users. Table II gives the spreading codes assigned to the users in the tests. The experimental results agree with the simulations.

In these tests, the delays and relative phases were kept constant. Other tests show a good fit between experimental and simulation results resembling those in Fig. 15. Similar tests were performed for the noncoherent receiver. These experimental results also agree with those obtained via simulation.

Fig. 16 shows BER results obtained for various trials with different delays and phases for the four-user case with the coherent version of the receiver. This figure shows that the real-time DSP implementation of the parallel partial inter-

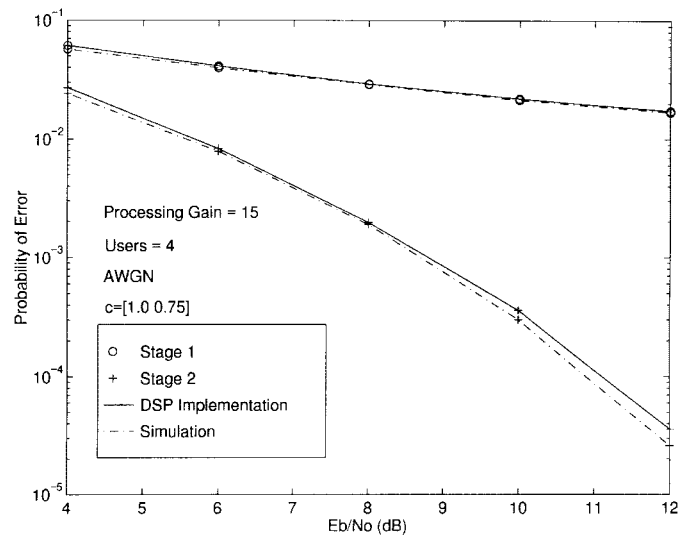


Fig. 15. Probability of bit error versus E_b/N_o experimental and simulation results for a single trial of the coherent receiver's DSP implementation ($N = 15$, with $C_k^{(2)} = 0.75$).

TABLE II
SPREADING SEQUENCES USED IN THE HARDWARE
TESTS OF THE MULTIUSER RECEIVER

	Spreading Sequence
User 1	1 1 0 0 1 0 1 1 1 1 0 1 0 0 1
User 2	1 1 1 1 0 0 0 1 0 0 0 1 1 0 1
User 3	0 1 0 0 0 1 0 0 1 0 0 0 1 0 1
User 4	1 0 1 0 1 1 1 1 1 0 1 0 1 0 0

ference cancellation receiver provides significant gains in performance. Improvement exceeds over one order of magnitude at $E_b/N_o = 10$ dB, compared to the conventional receiver for DS-CDMA. Analytical results based on the assumption of unbiased estimation [21] give optimistic results. BER results for the noncoherent receiver for the four-user case are presented in Fig. 17. These results also show a consequential performance improvement.

In all of these tests, synchronization is performed only on user 1. Perfect knowledge of the relative delays and phases with respect to user 1 was made available to the receiver. (The noncoherent receiver was not provided with side phase information.) In this paper, the effects of imperfect phase and timing estimation are not addressed. However, it has been shown analytically and via simulations that this structure is robust to phase estimation and synchronization errors [7].

Another version of the system has been successfully used to emulate the transmission of JPEG files over AWGN channels. In order to show the improved performance of the DSP implementation of the multiuser receiver, a JPEG file was jointly transmitted by four users. Each of the users was given one bit of the JPEG file in a round-robin fashion for transmission. At the receiver, the file was reassembled. The reconstructed JPEG file gives a sense of the average performance of the system across all users. Fig. 18 shows the reconstructed signal obtained from data estimated using

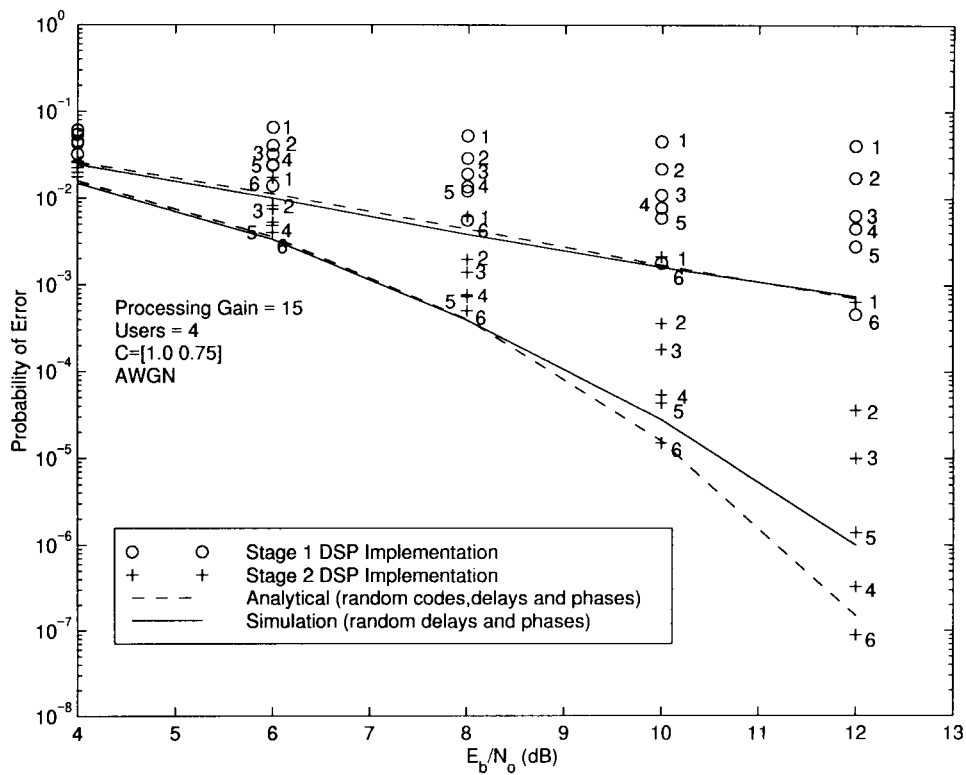


Fig. 16. Probability of bit error versus E_b/N_0 from real-time BER measurement results for the coherent multiuser receiver, simulated curves for random delays and phases, and analytical curves assuming unbiased estimation ($N = 15$, with $C_k^{(1)} = 1.0$ and $C_k^{(2)} = 0.75$).

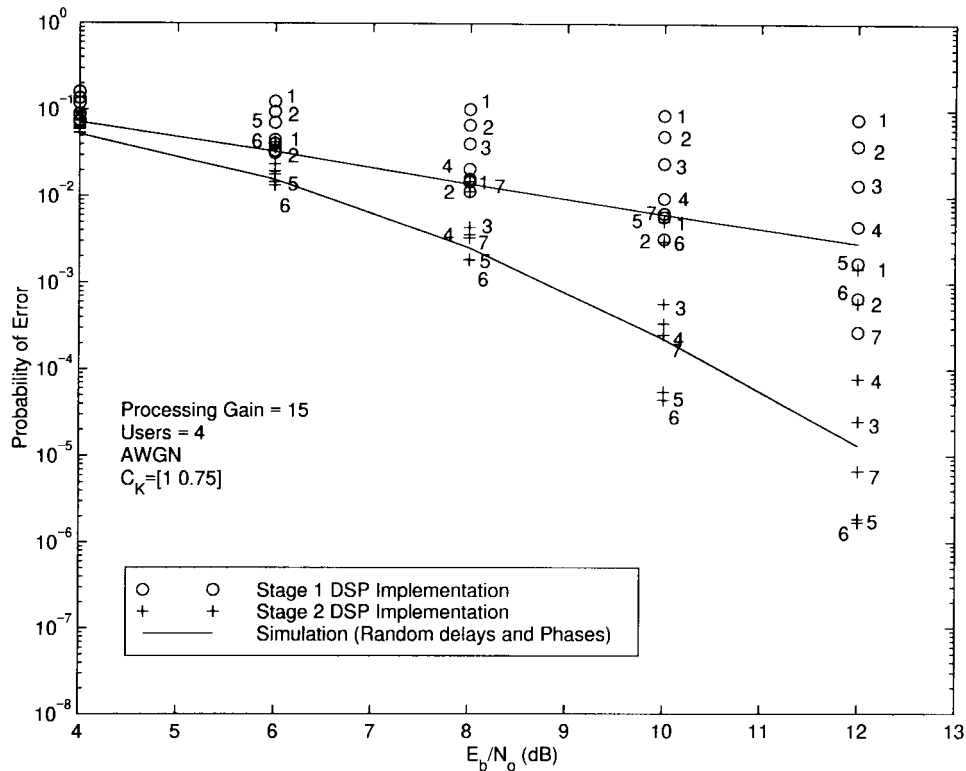


Fig. 17. Probability of bit error versus E_b/N_0 from real-time BER measurement results for the noncoherent receiver, simulated curves for random delays and phases, and analytical curves assuming unbiased estimation ($N = 15$, with $C_k^{(1)} = 1.0$ and $C_k^{(2)} = 0.75$).



Fig. 18. Reconstructed JPEG file from data estimated by the conventional coherent CDMA receiver ($E_b/N_o = 10$ dB, $N = 15$).



Fig. 19. Reconstructed JPEG file from data estimated by the coherent partial parallel interference cancellation receiver ($E_b/N_o = 10$ dB, $N = 15$, with $C_k^{(1)} = 1.0$ and $C_k^{(2)} = 0.75$).

the coherent conventional receiver for a four-user system operating at an $E_b/N_o = 10$ dB. Fig. 19 shows the JPEG file reconstructed from the estimates obtained in real time for the coherent partial parallel interference cancellation approach.

VII. CONCLUSIONS

Recent technological advances are making advanced DS-CDMA multiuser receivers practical. A real-time DSP-based parallel partial interference cancellation receiver has been successfully implemented, and its performance has been experimentally tested in AWGN channels. The implementation is based on a low-complexity approach to interference cancellation using the decision statistics from the previous stage of cancellation and a correction factor obtained from a residual signal that is common to all users to generate improved estimates. This approach reduces implementation complexity from quadratic to linear in the number of users with no penalties in performance. Experimental results confirm significant performance gains over the conventional receiver. The excellent tradeoff between complexity and performance offered by the parallel partial interference cancellation

technique and its affinity to the conventional receiver makes it an attractive approach for practical implementation in systems that exploit multiuser detection.

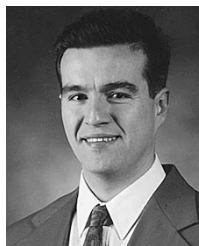
ACKNOWLEDGMENT

The authors would like to thank D. Breslin for developing the multisensor testbed, and S. Nicoloso for his priceless contributions to this project.

REFERENCES

- [1] S. Verdu, "Minimum probability of error for asynchronous Gaussian multiple access channels," *IEEE Trans. Inform. Theory*, vol. IT-32, pp. 85–96, Jan. 1986.
- [2] S. Moshavi, "Multi-user detection for DS-CDMA communications," *IEEE Commun. Mag.*, pp. 124–136, Oct. 1996.
- [3] A. Duel-Hallen, J. Holtzman, and Z. Zvonar, "Multiuser detection for CDMA systems," *IEEE Personal Commun.*, vol. 2, pp. 46–58, Apr. 1995.
- [4] J. D. Laster and J. H. Reed, "Interference rejection in wireless communications," *IEEE Commun. Mag.*, vol. 14, pp. 37–62, May 1997.
- [5] R. M. Buehrer, N. S. Correal, and B. D. Woerner, "A comparison of multiuser receivers for cellular CDMA," in *Proc. IEEE GLOBECOM*, Nov. 1996, pp. 1571–1577.
- [6] M. K. Varanasi and B. Aazhang, "Multistage detection in asynchronous code-division multiple access communications," *IEEE Trans. Commun.*, vol. 38, pp. 509–519, Apr. 1990.
- [7] R. M. Buehrer, A. Kaul, S. Striglis, and B. D. Woerner, "Analysis of DS-CDMA parallel interference cancellation with phase and timing errors," *IEEE J. Select. Areas Commun.*, vol. 14, pp. 1522–1535, Oct. 1996.
- [8] B. M. Leiner, R. J. Ruth, and A. R. Sastry, "Goals and challenges of the DARPA GloMo program," *IEEE Personal Commun.*, vol. 3, pp. 34–43, Dec. 1996.
- [9] S. F. Swachara, "An FPGA-based multiuser receiver employing parallel interference cancellation," M.S. thesis, Virginia Polytechnic Inst. State Univ., July 1998.
- [10] K. I. Pedersen, T. E. Kolding, I. Seskar, and J. M. Holtzman, "Practical implementation of successive interference cancellation in DS/CDMA systems," in *Proc., IEEE Int. Conf. Universal Personal Commun.*, 1996, pp. 321–325.
- [11] D. Dahlhaus, R. Heddergott, and M. Pesce, "A concept of a two-user CDMA hardware demonstrator for wireless outdoor communications," in *Proc. ACTS Mobile Commun. Summit*, Oct. 1997.
- [12] J. R. Lequepeys, N. Danielle, D. Lattard, B. Piaget, D. Varreau, L. Ouvry, and C. Boulanger, "CESSIUM: A single component for implementation of high data rates DSS/CDMA interference cancellation receivers," in *Proc. IEEE Int. Symp. Spread Spectrum Techniques Appl.*, Sept. 1998, pp. 663–667.
- [13] R. M. Buehrer and B. D. Woerner, "Analysis of adaptive multistage interference cancellation for CDMA using an improved Gaussian approximation," *IEEE Trans. Commun.*, vol. 44, pp. 1308–1320, Oct. 1996.
- [14] R. M. Buehrer, "The application of multiuser detection to cellular CDMA," Ph.D. dissertation, Virginia Polytechnic Inst. State Univ., 1996.
- [15] M. Latva-aho and J. Lilleberg, "Parallel interference cancellation in multiuser CDMA channel estimation," in *Wireless Personal Communications*. Norwell, MA: Kluwer Academic, 1998.
- [16] J. S. Lehnert and M. B. Pursley, "Error probabilities for binary direct-sequence spread-spectrum communications with random sequences," *IEEE Trans. Commun.*, vol. 37, pp. 1052–1061, Oct. 1989.
- [17] R. K. Morrow, Jr. and J. S. Lehnert, "Bit-to-bit error dependence in slotted DS/SSMA packet systems with random signature sequences," *IEEE Trans. Commun.*, vol. 37, pp. 1052–1061, Oct. 1989.
- [18] M. B. Pursley, "Performance evaluation for phase-coded spread-spectrum multiple-access communication—Part I: System analysis," *IEEE Trans. Commun.*, vol. COM-25, pp. 795–799, Aug. 1977.
- [19] A. J. Viterbi, *CDMA—Principles of Spread Spectrum Communication*. Reading, MA: Addison-Wesley, 1995.
- [20] D. Divsalar and M. Simon, "Improved CDMA performance using parallel interference cancellation," *Tech. Rep. 95-21*, JPL, Oct. 1995.
- [21] A. Kaul and B. D. Woerner, "An analysis of adaptive multistage interference cancellation for CDMA," in *Proc. IEEE Veh. Technol. Conf.*, 1994, pp. 82–26.

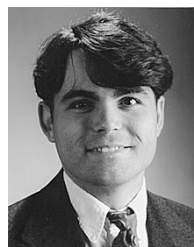
- [22] D. Divsalar, M. K. Simon, and D. Raphaeli, "Improved parallel interference cancellation for CDMA," *IEEE Trans. Commun.*, vol. 46, pp. 258–268, Feb. 1998.
- [23] T. S. Rappaport, S. Y. Seidel, and R. Singh, "900-MHz multipath propagation measurements for U.S. digital cellular radiotelephone," *IEEE Trans. Veh. Technol.*, vol. 39, pp. 132–139, Feb. 1990.
- [24] P. G. Renucci and B. D. Woerner, "Optimization of soft cancellation for DS-CDMA," *Electron. Lett.*, vol. 34, pp. 731–733, Apr. 1998.
- [25] Z. Zvonar and D. Brady, "Coherent and differentially coherent multiuser detectors for asynchronous CDMA frequency-selective channels," in *Proc. IEEE MILCOM*, Nov. 1992, pp. 442–446.
- [26] M. K. Varanasi, "Noncoherent detection in asynchronous multiuser channels," *IEEE Trans. Inform. Theory*, vol. 39, pp. 157–176, Jan. 1993.
- [27] P. Patel and J. Holtzman, "Analysis of a simple successive interference cancellation scheme in a DS/CDMA system," *IEEE J. Select. Areas Commun.*, vol. 12, pp. 796–807, June 1994.
- [28] D. F. Breslin, "Adaptive antenna arrays applied to position location," M.S. thesis, Virginia Polytechnic Inst. State Univ., Aug. 1997.
- [29] J. A. Wepman, "Analog and digital converters and their applications in radio receivers," *IEEE Commun. Mag.*, vol. 33, pp. 39–54, May 1995.
- [30] M. E. Frerking, *Digital Signal Processing in Communication Systems*. New York: Chapman and Hall, 1994.
- [31] C. Olmstead and M. Petrowski, "Digital IF processing," *RF Design*, pp. 34–40, Sept. 1994.
- [32] R. A. Cameron, "Fixed point implementation of a multistage receive," Ph.D. dissertation, Virginia Polytechnic Inst. State Univ., 1997.
- [33] R. Cameron and B. D. Woerner, "Synchronization of CDMA systems employing interference cancellation," in *Proc. IEEE Veh. Technol. Conf.*, 1996, pp. 178–182.



Neiyer S. Correal (S'94) was born in Bogota, Colombia, on November 26, 1968. He received the B.S. degree in electronics engineering from the Pontifical Javeriana University, Colombia, in 1992, and the M.S. degree in electrical engineering from Old Dominion University, VA, in 1994, where he was involved with real-time automatic speech recognition at the Speech Communication and Signal Processing Laboratory.

He is currently with the Mobile and Portable Radio Research Group (MPRG) at Virginia Polytechnic Institute and State University (Virginia Tech), where he is pursuing the Ph.D. degree. His research interests include spread-spectrum communications, multiuser detection, real-time signal processing, and implementation of advanced digital radio transceivers.

Mr. Correal is a member of Eta Kappa Nu and Tau Beta Pi.



R. Michael Buehrer (M'89) was born in Toledo, OH, on February 7, 1969. He received the B.S.E.E. and M.S.E.E. degrees from the University of Toledo in 1991 and 1993, respectively, where he specialized in satellite communications, and the Ph.D. degree from Virginia Polytechnic and State University in 1996, where he studied under a Bradley Fellowship.

During 1994 and 1995, he worked as a Systems Engineer at Stanford Telecommunications in the Advanced Programs Department in Reston, VA.

While at Virginia Tech, he worked with the Mobile and Portable Radio Research Group (MPRG) in the area of multiuser reception, spread spectrum applied to CDMA, and mobile radio. In particular, he specialized in interference cancellation techniques for cellular CDMA systems. In August 1996, he joined Bell Laboratories' Wireless Communication Laboratory as a Member of Technical Staff, where he has worked on advanced modulation and access techniques for ISM band communication. He is currently a member of the Wireless Signal Processing Group and is working on interference cancellation and adaptive antenna algorithms for second- and third-generation cellular systems.



Brian D. Woerner (S'87–M'87) was born on October 11, 1964. He received the B.S. degree in computer and electrical engineering from Purdue University, West Lafayette, IN, in 1986, and the M.S. and Ph.D. degrees from the University of Michigan, Ann Arbor, in 1987 and 1991, respectively, where he was a Unisys Fellow. He also received the Master of Public Policy degree from the University of Michigan's School of Public Policy Studies, with an emphasis in telecommunications policy.

He is an Associate Professor in the Bradley Department of Electrical Engineering at Virginia Tech University, Blacksburg. He is the current Director of the Mobile and Portable Radio Research Group (MPRG), and has been a member of this group since joining Virginia Tech in 1991.